



## Electrochemical behaviors and electrolytic separation of Th(IV) and Ce(III) in ThF<sub>4</sub>-CeF<sub>3</sub>-LiCl-KCl quaternary melt

Xianbin Wang<sup>a,b,c,1</sup>, Haiyang Zheng<sup>a,c,1</sup>, Qianhui Xu<sup>a,b,c</sup>, Tiejian Zhu<sup>a,c</sup>, Feng Jiang<sup>a,c</sup>, Changfeng She<sup>a,c</sup>, Chenyang Wang<sup>a,c</sup>, Haixia Cong<sup>a,b,c</sup>, Yu Gong<sup>a,c</sup>, Wei Huang<sup>a,c,\*</sup>, Qingnuan Li<sup>a,c,\*</sup>

<sup>a</sup> Shanghai Institute of Applied Physics, Chinese Academy of Sciences, Shanghai 201800, China

<sup>b</sup> University of Chinese Academy of Sciences, Beijing 100049, China

<sup>c</sup> Center of Excellence TMSR Energy System, Chinese Academy of Sciences, Shanghai 201800, China

### ARTICLE INFO

#### Keywords:

ThF<sub>4</sub>  
CeF<sub>3</sub>  
LiCl-KCl  
Electrolytic separation  
Pulse potential electrolysis

### ABSTRACT

The extraction and recycle of thorium is an essential step in the thorium-uranium closed fuel cycle designed for Thorium-based Molten Salt Reactor system (TMSR), and the separation of thorium from FPs especially lanthanides is a key issue in the thorium recovery. In this paper, the electrochemical behaviors of Th(IV) and Ce(III) on Mo electrode were studied by cyclic voltammetry (CV) and chronopotentiometry (CP) techniques at 773 K in ThF<sub>4</sub>(3 wt%)/CeF<sub>3</sub>(0.3 wt%)-LiCl-KCl ternary melt and CeF<sub>3</sub>(0.3 wt%)-ThF<sub>4</sub>(3 wt%)-LiCl-KCl quaternary melt, respectively. The reduction peaks of Th(IV)/Th(0) and Ce(III)/Ce(0) were at  $-1.83$  V and  $-2.21$  V (vs. Ag/AgCl) in the respective ternary melt, respectively, which were same with the values in the quaternary melt; however, the oxidation peaks in the CeF<sub>3</sub>-ThF<sub>4</sub>-LiCl-KCl melt shifted negatively about 0.1 V. Pulsed potential electrolysis of quaternary melt revealed that 98.9% of Th(IV) can be electrochemical separated from the melt with almost all cerium remaining in the melt, based on the inductively coupled plasma atomic emission spectrometer (ICP-AES) results.

### 1. Introduction

The effective utilization of thorium resource is an important goal for the Thorium-based Molten Salt Reactor system (TMSR) under developing in China, [1] and in the fuel reprocessing flowsheet for TMSR proposed by Shanghai Institute of Applied Physics (SINAP), fluoride volatility, low-pressure distillation and electrochemical separation methods were selected to recover uranium, carrier salt and thorium accordingly [2,3]. The residues of the fuel salt after fluoride volatility and distillation were mainly thorium and fission products (FPs) in the fluoride form. In this case, the electrochemical separation of thorium from fission products (FPs) especially lanthanides became a key issue in thorium recovery in the above flowsheet. Among the molten salt electrolytes, LiCl-KCl melt was more promising than fluoride melts because of its lower melting point and the larger gap in the reduction potential between actinides and lanthanides [4–12]. Therefore, LiCl-KCl melt had been proposed as the medium for the electrochemical separation of Th from fission products in the TMSR fuel reprocessing flowsheet [2,3].

In our previous works, we studied the electrochemical behaviors of

Th(IV) and Ln(III) in ThF<sub>4</sub>/LnF<sub>3</sub>(3 wt%)-LiCl-KCl ternary melt, and found that the existence of F<sup>-</sup> had no significant influence on the reduction reaction of Th(IV) and Ln(III) on the inert electrode under experimental conditions [3,13]. Compared with pure chlorides melts, the diffusion coefficients of Th(IV) and Ln(III) reduced in varying degree due to the strong Th-F/Ln-F interaction and the larger size of fluoride complexes, and similar results could also be found in other literature [14,15]. The difference of deposition potential between Th(IV) and Ln(III) in ThF<sub>4</sub>/LnF<sub>3</sub>-LiCl-KCl melt was more than 0.35 V (vs. Ag/AgCl), [3,13] which was well over the minimum potential difference (0.19 V) required for separation of An(IV) and Ln(III) [16]. So, it was reasonable to believe that ThF<sub>4</sub> can be electrochemically separated from LnF<sub>3</sub> in the LiCl-KCl melt.

In the present work, the electrode process of Th(IV) and Ce(III) in ThF<sub>4</sub>-CeF<sub>3</sub>-LiCl-KCl quaternary melt was studied by cyclic voltammetry (CV) and chronopotentiometry (CP), and the electrochemical separation of thorium and cerium from ThF<sub>4</sub>-CeF<sub>3</sub>-LiCl-KCl melt was also conducted by pulsed potential electrolysis.

\* Corresponding authors at: Shanghai Institute of Applied Physics, Chinese Academy of Sciences, Shanghai 201800, China.

E-mail addresses: [huangwei@sinap.ac.cn](mailto:huangwei@sinap.ac.cn) (W. Huang), [liqingnuan@sinap.ac.cn](mailto:liqingnuan@sinap.ac.cn) (Q. Li).

<sup>1</sup> The authors contributed equality.

## 2. Experiment

### 2.1. Agents and materials

The LiCl, KCl and  $\text{CeF}_3$  used in the experiment were purchased from Sigma-Aldrich, and the purity was 99.99%.  $\text{ThF}_4$  (99.9%) was provided by the Changchun Institute of Applied Chemistry (CAS) and dehydrated at 200 °C for 20 h before use. The Mo wire ( $\phi 1 \times 1.5$  mm, 99.99%) used as working electrode (WE) was purchased from Alfa-Aesar company. The counter electrode (CE) was spectrum pure graphite rod ( $\phi 3 \times 50$  mm) and purchased from Mersen Co., Ltd. The Ag/AgCl (5 mol%)-LiCl-KCl reference electrode was fabricated following the patent protocol [17].

### 2.2. Melt preparation

All the experiment were carried out in an electrical furnace which was connected with an argon glove box, and the maximum temperature of the furnace was 1273 K [18,19]. The preparation of LiCl-KCl (59:41 mol%) eutectic was performed following the procedure as reported in our previous work [3].

$\text{ThF}_4/\text{CeF}_3$ -LiCl-KCl ternary melt preparation: a certain amount of  $\text{ThF}_4$  or  $\text{CeF}_3$  powder and LiCl-KCl eutectic powder were mixed evenly and put into an alumina crucible, and then placed in the furnace. The concentration of  $\text{ThF}_4$  and  $\text{CeF}_3$  were fixed at 3 wt% and 0.3 wt%, respectively. After that, the furnace was sealed and heated to 573 K for 2 h, and then heated up to 823 K in 1 h and kept for 5 h. At last the melts were cooled to 573 K and solidified. The process of melting and solidification was repeated to make the dissolution of  $\text{ThF}_4$  and  $\text{CeF}_3$  completely. The prepared melt was kept at the experimental temperature for electrochemical analysis, or naturally cooled and grinded to powder for further use.

$\text{ThF}_4$ - $\text{CeF}_3$ -LiCl-KCl quaternary melt preparation: a certain amount of  $\text{CeF}_3$  was added into the prepared  $\text{ThF}_4$  (3 wt%)-LiCl-KCl powder, and the  $\text{CeF}_3$  concentration was 0.3 wt%. The mixture was heated to 573 K for 2 h in an alumina crucible under argon atmosphere in order to remove the trace water, and then heated to 773 K and kept 12 h before the following electrochemical experiments.

### 2.3. Electrochemical analysis and electrolysis of the melts

In the electrochemical analysis, the working electrode was inserted into the molten salt and the insertion depth was 5–10 mm. All the electrochemical experiments were carried out by an AUTOLAB PGSSTAT 302N workstation with the software Nova 1.9. The electrochemical behaviors of Th(IV) and Ce(III) in ternary and quaternary melts were investigated by the cyclic voltammetry (CV) and chronopotentiometry (CP) methods. The potentials in this work were measured by the Ag/AgCl (5 mol%) reference except those specifically noted.

The electrolysis of Th(IV) in  $\text{ThF}_4$ - $\text{CeF}_3$ -LiCl-KCl quaternary melt was carried out by pulse potential method [3,20]. Each pulse process consists of four stages, and the mechanism of them had been described in the literatures previously [3]. The concentration of Th and Ce in the molten salt before and after electrolysis was analyzed by the inductively coupled plasma atomic emission spectrometer (ICP-AES, Optima 8000 produced by Perkin Elmer), and the electrolysis products were characterized by the X-ray diffraction (XRD, X'PERT PRO MPD produced by Panalytical).

## 3. Results and discussion

### 3.1. The electrochemical behaviors of Th(IV) and Ce(III) in the $\text{ThF}_4/\text{CeF}_3$ -LiCl-KCl ternary melt

Fig. 1a was the CV curves of LiCl-KCl and  $\text{CeF}_3$ (0.3 wt%)-LiCl-KCl

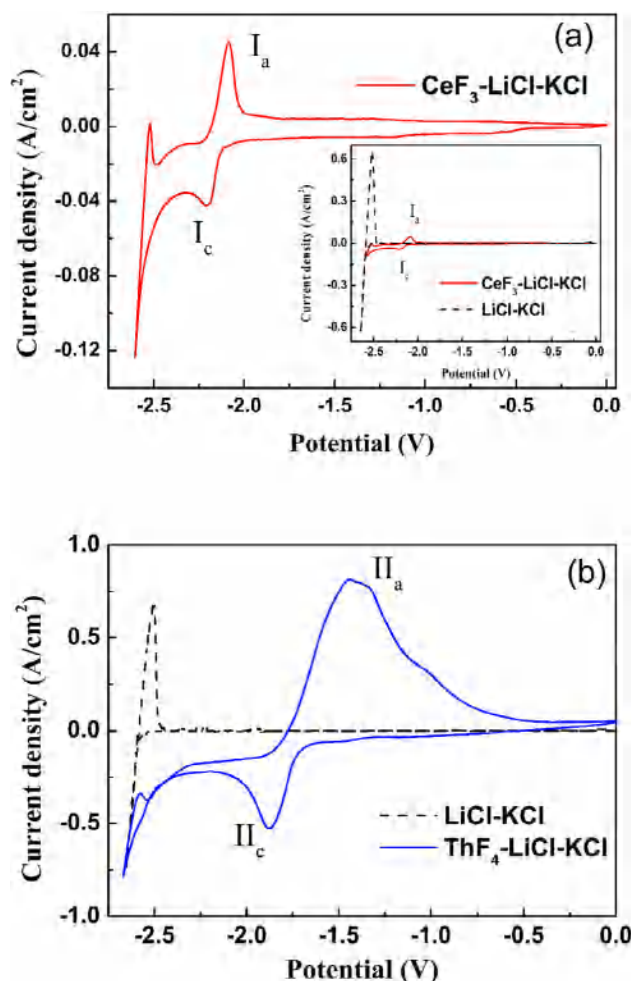


Fig. 1. Cyclic voltammograms of LiCl-KCl eutectic &  $\text{CeF}_3$ (0.3 wt%)-LiCl-KCl (a) and LiCl-KCl eutectic &  $\text{ThF}_4$ (3 wt%)-LiCl-KCl (b) melts on a Mo electrode at 773 K. Electrode area  $S = 0.23 \text{ cm}^2$  (a) and  $0.30 \text{ cm}^2$  (b), scan rate:  $100 \text{ mV s}^{-1}$ , auxiliary electrode: graphite rod ( $\Phi 3 \times 50$  mm), reference electrode: Ag/AgCl (5 mol%).

melts in the potential range of 0 to  $-2.65$  V at 773 K. In the illustration of Fig. 1a, the black dotted line was the CV curve of the blank LiCl-KCl melt, and only a pair of reduction and oxidation peaks at about  $-2.60$  V were observed. The red solid line was the CV signal obtained from  $\text{CeF}_3$ (0.3 wt%)-LiCl-KCl melt. Compared with the blank melt, another pair of reduction and oxidation signals located at about  $-2.21$  V ( $I_c$ ) and  $-2.08$  V ( $I_a$ ) appeared in the CV curve. As the reduction occurred, the current rapidly increased and slowed down, which was a typical reaction of new phase generation [21]. This phenomenon was consistent with that in the  $\text{CeF}_3$ (3 wt%)-LiCl-KCl melt, [13] and based on the peak potential against Ag/AgCl, the relationship between peak potentials and their attributions in this work had been listed and compared with those in the literature, as shown in Table 1. The results

Table 1

The relationship between peak potentials and their attributions in cyclic voltammograms in this work (Fig. 1) and literature.

Peak attributions	Peak potentials (V) in this work (vs. Ag/AgCl)	Peak potentials (V) in literature (vs. Ag/AgCl)
$\text{Ce(III)} + 3e^- \rightarrow \text{Ce}$	$I_c$ -2.21	-2.21 [13]
$\text{Ce} \rightarrow \text{Ce(III)} + 3e^-$	$I_a$ -2.08	2.00 [13]
$\text{Th(IV)} + 4e^- \rightarrow \text{Th}$	$II_c$ -1.87	-1.83 [3]
$\text{Th} \rightarrow \text{Th(IV)} + 4e^-$	$II_a$ -1.44	-1.46 [3]

revealed that peak I<sub>c</sub> and I<sub>a</sub> in Fig. 1a should be attributed to the reduction of Ce(III) to metal Ce and the dissolution of metal Ce to Ce(III), respectively.

Fig. 1b was the CV curve of the ThF<sub>4</sub>(3 wt%)-LiCl-KCl melt obtained in the potential range of 0 to -2.65 V at 773 K, and a pair of reduction and oxidation signals located at about -1.87 V (II<sub>c</sub>) and -1.44 V (II<sub>a</sub>), which were also consistent with our previous report [3]. Similarly, according to the data in Table 1, the reduction (II<sub>c</sub>) and oxidation (II<sub>a</sub>) peaks corresponded to the Th(IV) reduction to metal and the Th metal dissolution to Th(IV) on the Mo electrode, respectively.

In the process of electrolysis, the theoretical extraction rate of elements, the deposition potentials and the transfer electron number of the electrochemical reduction reaction have the following relation [5]:

$$\Delta E = \frac{RT}{nF} \ln \frac{1}{1-\eta} \quad (1)$$

Among them,  $\Delta E$  is the difference between the electrolysis potential and the standard deposition potential of the ions,  $R$  is the gas constant,  $F$  is Faraday's constant,  $n$  is the number of transfer electron reaction,  $T$  is the temperature in K, and  $\eta$  is the theoretical extraction rate of a certain element. For Th-Ce system, the theoretical extraction rate and the difference of their deposition potentials have the following relation (in which  $\alpha$  is the activity of ions):

$$\Delta E_{Th-Ce} = E_{Th(IV)/Th}^{\#0} - E_{Ce(III)/Ce}^{\#0} \geq \frac{RT}{3F} \ln \alpha_{Ce(III)} (1-\eta_{Ce}) - \frac{RT}{4F} \ln \alpha_{Th(IV)} (1-\eta_{Th}) \quad (2)$$

According to Eq. (2), on the condition of the assumption that  $\alpha_{Th(IV)}$  and  $\alpha_{Ce(III)}$  are 1 and  $\eta_{Ce}$  is 0.01%, when the potential difference of two elements is more than 0.19 V and the temperature is 773 K, the theoretical extraction rate of 4 electrons transfer electrochemical reaction, such as  $Th(IV) + 4e^- \rightarrow Th$ , can reach a value as high as 99.999% (for a 3 electrons reaction, this value will be 99.98%) [12,16]. As discussed above, the difference between the reduction potential of Th(IV) and Ce(III) in the LiCl-KCl melt is about 0.38 V, so it is feasible to realize the separation of these two elements by electrolysis.

### 3.2. The electrochemical behaviors of Th(IV) and Ce(III) in the CeF<sub>3</sub>-ThF<sub>4</sub>-LiCl-KCl quaternary melt

In order to optimize the electrolysis parameters, CV measurement of Ce(III) and Th(IV) in the CeF<sub>3</sub>-ThF<sub>4</sub>-LiCl-KCl quaternary melt was carried out before the implementation of electrolytic operation, and the results were shown in Fig. 2. Compared with the results of CeF<sub>3</sub>-LiCl-KCl and ThF<sub>4</sub>-LiCl-KCl ternary melts, the CV curve of the CeF<sub>3</sub>-ThF<sub>4</sub>-

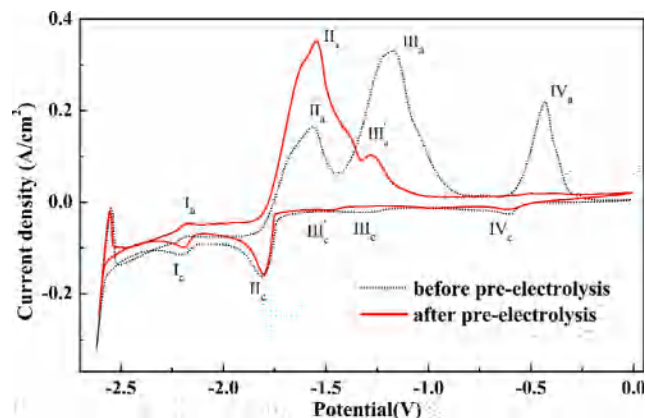
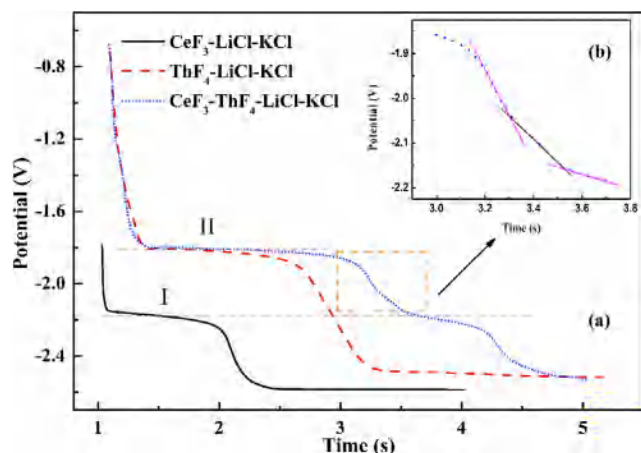


Fig. 2. Cyclic voltammograms of CeF<sub>3</sub>(0.3 wt%)-ThF<sub>4</sub>(3 wt%)-LiCl-KCl melt on a Mo electrode ( $S = 0.35 \text{ cm}^2$ ) at 773 K before and after pre-electrolysis. Scan rate:  $100 \text{ mV s}^{-1}$ , auxiliary electrode: graphite rod ( $\Phi 3 \times 50 \text{ mm}$ ), reference electrode: Ag/AgCl (5 mol%).

LiCl-KCl quaternary melt was more complex, as presented in the black dashed line in Fig. 2. In the cathodic scan of the CV curve from 0 to -2.60 V, except for the reduction peak of the electrochemical window of LiCl-KCl melt, there were four obvious reduction peaks labeled as IV<sub>c</sub>, III<sub>c</sub>, II<sub>c</sub> and I<sub>c</sub>, which were located at about -0.61 V, -1.30 V, -1.81 V and -2.20 V, respectively. II<sub>c</sub> and I<sub>c</sub> corresponded to the reduction of Th(IV)  $\rightarrow$  Th and Ce(III)  $\rightarrow$  Ce on the Mo electrode, respectively, and the peak potentials were consistent with the individual solute in the ternary melt. In the anodic scan, four oxidation peaks appeared, namely I<sub>a</sub>, II<sub>a</sub>, III<sub>a</sub> and IV<sub>a</sub>. The oxidation peak I<sub>a</sub> ( $\sim -2.18 \text{ V}$ ) was related to I<sub>c</sub> and could be assigned to the oxidation of Ce metal; similarly, II<sub>a</sub> ( $\sim -1.56 \text{ V}$ ) was related to II<sub>c</sub> and could be attributed to the oxidation of Th metal. Compared to the ternary melts in Fig. 1, I<sub>a</sub> and II<sub>a</sub> in Fig. 2 had a negative shift of about 0.1 V, which could be ascribed to the reduction products dissolution on the deposited Th-Ce alloy layer of the Mo electrode; in the more positive potential range, there were two intense oxidation peaks near -1.17 V and -0.43 V, namely III<sub>a</sub> and IV<sub>a</sub>, which corresponded to III<sub>c</sub> and IV<sub>c</sub>. The unsorted couples of III<sub>c</sub>/III<sub>a</sub> and IV<sub>c</sub>/IV<sub>a</sub> might be caused by the impurities in the melt.

In order to exclude the interference of impurities and confirm the attribution of III<sub>c</sub>/III<sub>a</sub> and IV<sub>c</sub>/IV<sub>a</sub>, the melt was pretreated by a potentiostatic electrolysis purification for 2 h at the potential of -1.6 V (slightly positive to the reduction potential of Th(IV)). The CV curve of the pre-electrolyzed CeF<sub>3</sub>-ThF<sub>4</sub>-LiCl-KCl quaternary melt was also shown in the red solid line of Fig. 2. Compared with the curve before pre-electrolysis, the peak IV<sub>c</sub> decreased and IV<sub>a</sub> almost disappeared, indicating the couple of IV<sub>c</sub>/IV<sub>a</sub> were assigned to some impurity except Ce(III) and Th(IV) in the melt and the concentration decreased remarkably after pre-electrolysis. Also, the couple of III<sub>c</sub>/III<sub>a</sub> decreased and their peak potential shifted negatively after pre-electrolysis (III<sub>c</sub> shifted from -1.30 V to -1.48 V (III<sub>c</sub>'), and III<sub>a</sub> shifted from -1.17 V to -1.28 V (III<sub>a</sub>')), revealing that this pair of peaks might be related to the reduction deposition and oxidation dissolution of the alloy formed by the co-reduction of Th(IV) and impurities. However, the oxidation peak of Th after pre-electrolysis (II<sub>a</sub>') was higher than that before pre-treated (II<sub>a</sub>), implied the generation of Th metal increased while the concentration of impurities and the formation of Th alloy decreased after pre-electrolysis. According to the literature, [22] the potential of the reduction of Cu(I) on the Mo electrode in the CuCl-LiCl-KCl melt was near -0.6 V. In this experiment, Cu metal was used as the fixture of the electrodes and conductor wire, and could be oxidized and then dissolved in the melt at the high temperature. Actually, the ICP-AES analysis of the melt showed that the Cu concentration decreased significantly after pre-electrolysis (from 14.3 ppm to 0.2 ppm). As a result, it can be concluded that IV<sub>c</sub>/IV<sub>a</sub> in the CV curve probably corresponds to the redox process of the Cu(I) impurity from the corrosion of Cu accessory, and III<sub>c</sub>/III<sub>a</sub> is assigned to the generation and dissolution of the small amount Th-Cu alloy deposited on the electrode.

Fig. 3 was the CP curves obtained from the above three kinds of melts. For ThF<sub>4</sub>-LiCl-KCl ternary system, a platform (II) appeared near -1.81 V, indicating the reduction of Th(IV) occurred at this potential, which was coincident with the results of CV. Similarly, the platform (I) near -2.18 V in the CP curve of CeF<sub>3</sub>-LiCl-KCl ternary melt implied the reduction of Ce(III), also very consistent with the above CV results. In the CeF<sub>3</sub>-ThF<sub>4</sub>-LiCl-KCl quaternary melt (after pre-electrolysis), two obvious platforms near -1.81 V and -2.18 V were observed, which corresponded to the reduction of Th(IV) and Ce(III), respectively. The potential values of platforms location were almost the same as those of the ternary melts. Furthermore, two smallish platforms between -1.90 V to -2.16 V were found, as shown in the insert of Fig. 3. This result suggested that reduction reactions occur in this potential range between the reduction of Th(IV) and Ce(III), which could be inferred to the deposition of Ce on the surface of metal Th or the generation of Th-Ce alloys. However, no significant correlative reduction peaks were observed in cyclic voltammograms in Fig. 2, which could be due to the



**Fig. 3.** Chronopotentiograms of  $\text{CeF}_3(3 \text{ wt}\%)\text{-LiCl-KCl}$ ,  $\text{ThF}_4(3 \text{ wt}\%)\text{-LiCl-KCl}$  and  $\text{CeF}_3(0.3 \text{ wt}\%)\text{-ThF}_4(3 \text{ wt}\%)\text{-LiCl-KCl}$  melts (after pre-electrolysis) on a Mo electrode ( $S = 0.23 \text{ cm}^2$ ,  $0.30 \text{ cm}^2$  and  $0.35 \text{ cm}^2$ , respectively) at 773 K. Applied current: 50 mA, auxiliary electrode: graphite rod ( $\Phi 3 \times 50 \text{ mm}$ ), reference electrode: Ag/AgCl (5 mol%).

relative lower concentration of Ce(III) in the melt and these reduction peaks were covered by those of Th(IV) deposition in the CV curves.

### 3.3. The electrolysis of Th(IV) in $\text{CeF}_3\text{-ThF}_4\text{-LiCl-KCl}$ quaternary melt

#### 3.3.1. Determination of electrolysis parameters

As shown in Section 3.2, the possible co-reduction of Ce(III) and Th(IV) and generation of Th-Ce alloys will lead to positive shift of the reduction potential of Ce(III), resulting in adverse effects of the separation of Th and Ce. Therefore, it is very important to choose the appropriate electrolysis procedures and parameters. In our previous work [3], an electrolysis method of pulsed potential was employed for the separation of Th from the LiCl-KCl melt and good results were achieved. In the present work, a similar pulse potential electrolysis procedure was employed for the Th(IV) separation in the  $\text{CeF}_3\text{-ThF}_4\text{-LiCl-KCl}$  quaternary melt and the parameters were optimized somewhat.

To maximize the separation rate of Th and minimize the extraction of Ce from the melt, the pulse electrolysis process was improved: the pulse potentials of the electrolysis (enrichment, electrolysis, dissolution and stabilization) were optimized and adjusted to  $-2.00 \text{ V}$ ,  $-1.90 \text{ V}$ ,  $-1.60 \text{ V}$  and  $-1.70 \text{ V}$ , respectively (see Fig. 4). Compared with the electrolysis procedure in  $\text{ThF}_4\text{-LiCl-KCl}$  melt, [3] the potential of

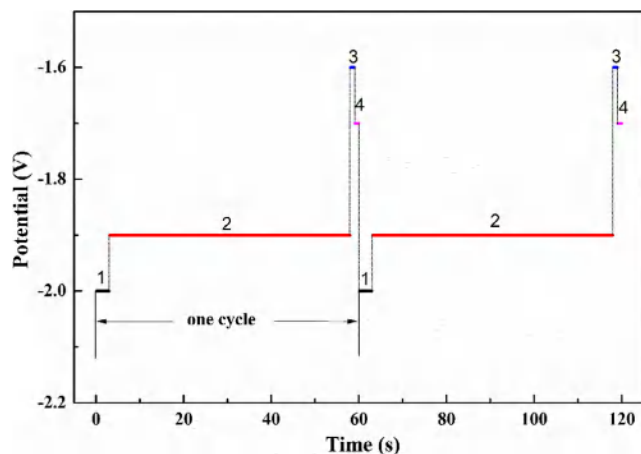


**Fig. 4.** Parameters applied in the pulse potential electrolysis of Th(IV) in the  $\text{CeF}_3(0.3 \text{ wt}\%)\text{-ThF}_4(3 \text{ wt}\%)\text{-LiCl-KCl}$  melt.

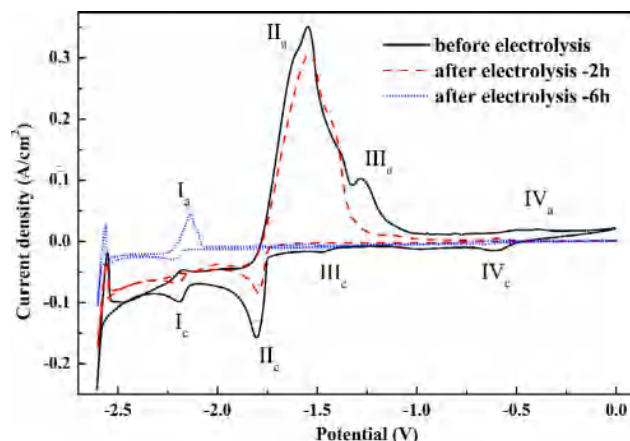


**Fig. 5.** Cyclic voltammograms of  $\text{CeF}_3(0.3 \text{ wt}\%)\text{-ThF}_4(3 \text{ wt}\%)\text{-LiCl-KCl}$  melt on Mo electrode ( $S = 0.35 \text{ cm}^2$ ) at scan rate of  $100 \text{ mV s}^{-1}$  before and after electrolysis at 773 K. Auxiliary electrode: graphite rod ( $\Phi 3 \times 50 \text{ mm}$ ), reference electrode: Ag/AgCl (5 mol%).

enrichment stage in this work increased from  $-2.35 \text{ V}$  to  $-2.00 \text{ V}$ , preventing the deposition of Ce on the electrode; the potential of dissolution stage shifted negatively from  $0.40 \text{ V}$  to  $-1.60 \text{ V}$ , which was slightly more positive than the deposition potential of Th(IV) ( $\sim -1.80 \text{ V}$ ) and could reduce the excessive dissolution of deposition from the electrode surface to the melt; the potential of stabilization stage was adjusted from  $0 \text{ V}$  to  $-1.70 \text{ V}$ , which was near the half-wave potential of the electrochemical reaction of Th(IV) ( $E_{1/2} = (E_{pa} + E_{pc})/2 \approx -1.69 \text{ V}$ ) with the balance of deposition of Th(IV) and dissolution of Th metal.

#### 3.3.2. Monitoring of electrolysis process

CV measurements were performed before and after electrolysis for the monitoring of the reaction progress in  $\text{CeF}_3\text{-ThF}_4\text{-LiCl-KCl}$  quaternary melt. Fig. 5 was the CV curves of the melt before and after electrolysis. Before electrolysis (black solid line), the redox peaks of Th(IV) ( $\text{II}_c$  &  $\text{II}_a$ ) and Ce(III) ( $\text{I}_c$  &  $\text{I}_a$ ) of CV curve were obvious and the signal intensity of  $\text{II}_c$  &  $\text{II}_a$  were large. Furthermore, the signals of impurity (the couples of  $\text{III}_c$  &  $\text{III}_a$  and  $\text{IV}_c$  &  $\text{IV}_a$ , as described in Section 3.2) were also clearly visible.

As the electrolysis continued, the signals of Th(IV) decreased gradually, and the peaks of impurity also weakened over time and finally disappeared, as shown in the red dashed and blue dotted line in Fig. 5. At the same time, the signal of Ce(III) became clearer and had little intensity changes. When the electrolysis proceeded to 6 h, the Th(IV) signals ( $\text{II}_c$  &  $\text{II}_a$ ) almost disappeared, and only the Ce(III) signals ( $\text{I}_c$  &  $\text{I}_a$ ) could be observed in the whole CV curve. The onset reduction potentials of Ce(III) were slightly shifted negatively with the duration time of electrolysis, and the detail changes were shown in Table 2. Meanwhile, the melt was sampled at different stages of electrolysis. The concentration of Th and Ce in the melt was analyzed by ICP-AES, and the results were shown in Table 3.

According to the results of Fig. 5 and Table 3, the concentration of Ce remained in the melt was almost the same during the electrolysis

**Table 2**

The onset reduction potentials of Th(IV) and Ce(III) of  $\text{CeF}_3(0.3 \text{ wt}\%)\text{-ThF}_4(3 \text{ wt}\%)\text{-LiCl-KCl}$  melt before and after electrolysis.

Electro-pairs	Onset reduction potential (V)		
	0 h	2 h	6 h
Th(IV)/Th	-1.75	-1.75	
Ce(III)/Ce	-2.13	-2.14	-2.17

**Table 3**

The concentration of thorium and cerium in the  $\text{CeF}_3(0.3 \text{ wt}\%)\text{-ThF}_4(3 \text{ wt}\%)\text{-LiCl-KCl}$  melt after different electrolysis time and the calculated separation ratio of thorium.

Electrolysis time (h)	Concentration of Th ( $\text{mol kg}^{-1}$ )	Concentration of Ce ( $\text{mol kg}^{-1}$ )	Calculated separation ratio of Th (%)
0	$7.92 \times 10^{-2}$	$1.46 \times 10^{-2}$	0
2	$3.98 \times 10^{-2}$	$1.48 \times 10^{-2}$	49.7
4	$6.21 \times 10^{-3}$	$1.51 \times 10^{-2}$	92.2
6	$9.17 \times 10^{-4}$	$1.47 \times 10^{-2}$	98.9

process, while the onset reduction potential shifted about 40 mV to the negative, which could be attributed to the relative increased concentration of  $\text{F}^-$  in the melt. As the electrolysis went on, the  $\text{Cl}^-$  was oxidized on the anode [15] and the concentration of  $\text{F}^-$  in the melt maintained stable. So, when Th(IV) was electrochemically deposited on the cathode and its concentration continually decreased, the fluorine ions complexed with Th(IV) were released into melt. After a 6 h-electrolysis, only 1% Th(IV) was left in the melt and the ratio of F/Ce was increased to about 25. This result led to the coordination of Ce(III) with  $\text{F}^-$  and the formation of more  $\text{CeF}_n^{(n-3)-}$  complex, and the decrease of diffusion coefficient of Ce (III), [23] just like the Th-Cl-F system in chlorides. [15,24] As a result, the concentration of free  $\text{Ce}^{3+}$  ion as well as the activity of Ce(III) decreased in the melt, and according to the Nernst equation the reduction potential of Ce(III) shifted negatively ( $\alpha$  is the activity of ions):

$$E^{eq} = E^0 + 2.303 \frac{RT}{nF} \log \alpha_{\text{Ce(III)}} \quad (3)$$

From Table 3, the separation rate of Th reached up to 98.9% when the  $\text{CeF}_3(0.3 \text{ wt}\%)\text{-ThF}_4(3 \text{ wt}\%)\text{-LiCl-KCl}$  melt was electrolyzed up to 6 h, which was much higher than that in a similar melt (86.8% in  $\text{ThF}_4(3 \text{ wt}\%)\text{-LiCl-KCl}$  melt with a duration time of 10 h) by the non-optimized pulse electrolysis procedure. [3]

### 3.3.3. Characterization of electrolysis products

The cathode deposition of  $\text{CeF}_3(0.3 \text{ wt}\%)\text{-ThF}_4(3 \text{ wt}\%)\text{-LiCl-KCl}$  quaternary melt after 6 h electrolysis was identified by XRD, and the cling film was employed to prevent the entrained molten salt from moisture absorption during testing. As shown in Fig. 6, the XRD pattern of untreated deposition indicated that it was mainly composed of Th metal, LiCl and KCl. However, due to the large amount of molten salt entrained in the deposition, the signals of Th metal were not clear enough to some extent. Therefore, a cathode product processing of

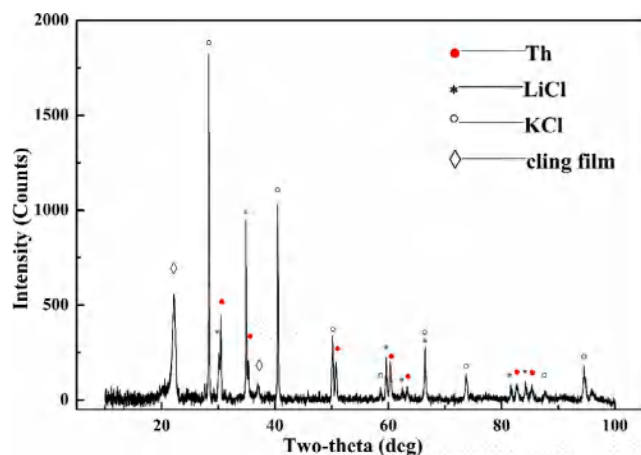


Fig. 6. XRD pattern of cathodic deposit obtained from  $\text{CeF}_3(0.3 \text{ wt}\%)\text{-ThF}_4(3 \text{ wt}\%)\text{-LiCl-KCl}$  melt on a spiral molybdenum electrode at 773 K for 6 h electrolysis (before distillation).

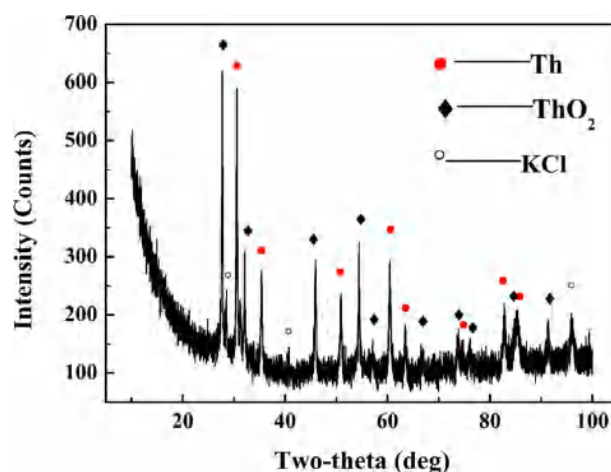


Fig. 7. XRD pattern of cathodic deposit obtained from  $\text{CeF}_3(0.3 \text{ wt}\%)\text{-ThF}_4(3 \text{ wt}\%)\text{-LiCl-KCl}$  melt on a spiral molybdenum electrode at 773 K for 6 h electrolysis (after distillation at 900 °C and 10 Pa).

distillation was employed at 900 °C and 10 Pa, and most of the molten salt was distilled from the deposition. The product after distillation was also characterized by XRD, as shown in Fig. 7. After distillation treatment, only few molten salt remained and the product contained two major substances namely Th metal and  $\text{ThO}_2$ . The occurrence of  $\text{ThO}_2$  probably arose from partial oxidation of Th metal during sample transfer and high-temperature distillation.

## 4. Conclusions

The electrochemical behaviors of Th(IV) and Ce(III) in  $\text{ThF}_4(3 \text{ wt}\%)\text{-CeF}_3(0.3 \text{ wt}\%)\text{-LiCl-KCl}$  ternary melt and  $\text{CeF}_3(0.3 \text{ wt}\%)\text{-ThF}_4(3 \text{ wt}\%)\text{-LiCl-KCl}$  quaternary melt at 773 K on Mo electrode were investigated by CV and CP techniques. The reduction peaks of Th(IV)/Th(0) and Ce(III)/Ce(0) were at  $-1.83 \text{ V}$  and  $-2.21 \text{ V}$  (vs. Ag/AgCl) in the respective ternary melt, respectively, which were same with the values in the quaternary melt; however, the oxidation peaks shifted negatively about 0.1 V in the quaternary melt, which could be ascribed to the reduction products dissolution on the Th-Ce alloy layer of the electrode. The separation rate of Th reached up to 98.9% when the duration time of electrolysis was up to 6 h by the optimized pulse electrolysis procedure, and the cathode product contained Th metal and  $\text{ThO}_2$ . The concentration of Ce in the quaternary melt remained almost the same during the electrolysis process with the onset reduction potential negative-shifting of about 40 mV, which could be attributed to the relative increased concentration of  $\text{F}^-$  in the melt. From the above results, we can conclude that  $\text{ThF}_4$  can be electrochemically separated from  $\text{CeF}_3$  (very likely including other lanthanide fluorides) in the LiCl-KCl melt, which will provide a scientific basis for the further research and development of effective Th electrolysis separation in the re-processing of MSR fuel.

## Acknowledgments

This work was supported by the “Strategic Priority Research Program” and “Frontier Science Key Program” of the Chinese Academy of Sciences (Grant No. XDA02030000 and QYZDYSSW-JSC016), National Natural Science Foundation of China (21601200) and Youth innovation Promotion Association of CAS (2017307).

## Appendix A. Supplementary material

Supplementary data associated with this article can be found, in the online version, at <https://doi.org/10.1016/j.seppur.2018.08.013>.

## References

- [1] H. Xu, Z. Dai, X. Cai, Some physical issues of the thorium molten salt reactor nuclear energy system, *Nucl. Phys. News* 24 (2014) 24–30.
- [2] Q. Li, Current progress in R&D on pyroprocess technology for TMSR in SINAP, *Int. Pyroprocess. Res. Conf.* 2014 (2014).
- [3] X. Wang, W. Huang, Y. Gong, F. Jiang, H. Zheng, T. Zhu, D. Long, Q. Li, Electrochemical behavior of Th(IV) and its electrodeposition from ThF<sub>4</sub>-LiCl-KCl melt, *Electrochim. Acta* 196 (2016) 286–293.
- [4] F.R. Clayton, G. Mamantov, D.L. Manning, Electrochemical studies of uranium and thorium in molten LiF-NaF-KF at 500 degrees C, *J. Electrochem. Soc.* 121 (1974) 86–90.
- [5] P. Chamelot, L. Massot, C. Hamel, C. Nourry, P. Taxil, Feasibility of the electrochemical way in molten fluorides for separating thorium and lanthanides and extracting lanthanides from the solvent, *J. Nucl. Mater.* 360 (2007) 64–74.
- [6] P. Chamelot, L. Massot, L. Cassayre, P. Taxil, Electrochemical behaviour of thorium (IV) in molten LiF-CaF<sub>2</sub> medium on inert and reactive electrodes, *Electrochim. Acta* 55 (2010) 4758–4764.
- [7] L. Cassayre, J. Serp, P. Soucek, R. Malmbeck, J. Rebizant, J.P. Glatz, Electrochemistry of thorium in LiCl-KCl eutectic melts, *Electrochim. Acta* 52 (2007) 7432–7437.
- [8] J.S. Zhang, Electrochemistry of actinides and fission products in molten salts-data review, *J. Nucl. Mater.* 447 (2014) 271–284.
- [9] G. Pakhui, M. Chandra, S. Ghosh, B.P. Reddy, K. Nagarajan, Electrochemical studies on the reduction behaviour of Th<sup>4+</sup> in molten LiCl-KCl eutectic, *Electrochim. Acta* 155 (2015) 372–382.
- [10] M. Straka, L. Szatmary, J. Subrt, Electrochemical and microscopic study of thorium in a molten fluoride system, *J. Electrochem. Soc.* 162 (2015) D449–D456.
- [11] Z.H. Wang, D. Rappleye, M.F. Simpson, Voltammetric analysis of mixtures of molten eutectic LiCl-KCl containing LaCl<sub>3</sub> and ThCl<sub>4</sub> for concentration and diffusion coefficient measurement, *Electrochim. Acta* 191 (2016) 29–43.
- [12] A.F. Laplace, J. Lacquement, J.L. Willit, R.A. Finch, G.A. Fletcher, M.A. Williamson, Electrodeposition of uranium and transuranics metals (Pu) on solid cathode, *Nucl. Technol.* 163 (2008) 366–372.
- [13] X. Wang, D. Long, T. Zhu, H. Zheng, F. Jiang, C. She, W. Huang, Q. Li, Electrochemical behaviors of Ln<sup>3+</sup> in LnF<sub>3</sub>-LiCl-KCl molten salt, *Nucl. Techniq.* 41 (2018) (in press).
- [14] P.J. Tumidajski, S.N. Flengas, Potential measurements of thorium tetrachloride in alkali-halide solutions, *Can. J. Chem.* 69 (1991) 462–467.
- [15] S. Delpéch, S. Jaskierowicz, D. Rodrigues, Electrochemistry of thorium fluoride in LiCl-KCl eutectic melts and methodology for speciation studies with fluorides ions, *Electrochim. Acta* 144 (2014) 383–390.
- [16] Y. Liu, G. Ye, Z. Chai, W. Shi, Research progress on molten salt electrorefining process by forming aluminum alloys, *J. Nucl. Radiochem.* 39 (2017) 13–21.
- [17] T. Zhu, H. Zheng, G. Zhang, W. Huang, D. Long, Q. Li, A Ag/AgCl reference electrode and its preparation method, *Chinese Patent ZL 1 (0494891)* (2014).
- [18] D. Long, W. Huang, F. Jiang, L. Tian, Q. Li, Study on the electrochemical extraction of rare earth elements from FLINAK, in: *GLOBAL 2013: International Nuclear Fuel Cycle Conference – Nuclear Energy at a Crossroads*, American Nuclear Society, Salt Lake City, 2013, pp. 411–418.
- [19] W. Huang, L. Tian, C. She, F. Jiang, H. Zheng, W. Li, G. Wu, D. Long, Q. Li, Electrochemical behavior of Europium(III)-Europium(II) in LiF-NaF-KF molten salt, *Electrochim. Acta* 147 (2014) 114–120.
- [20] M. Ueda, H. Kigawa, T. Ohtsuka, Co-deposition of Al-Cr-Ni alloys using constant potential and potential pulse techniques in AlCl<sub>3</sub>-NaCl-KCl molten salt, *Electrochim. Acta* 52 (2007) 2515–2519.
- [21] F. Gao, C. Wang, L. Liu, J. Guo, S. Chang, L. Chang, R. Li, Y. Ouyang, Electrode process of La(III) in molten LiCl-KCl, *J. Rare Earth* 27 (2009) 986–990.
- [22] Y. Cai, H. Liu, Q. Xu, Q. Song, L. Xu, Electrochemical behavior of copper in eutectic LiCl-KCl melt, *Nonferr. Metals (Extract. Metall.)* 8 (2015) 1–5.
- [23] J. Song, X. Zhang, A. Mukherjee, Electrochemical behaviors of Ce(III) in Molten AlCl<sub>3</sub>-NaCl under various contents of fluoride, *J. Electrochem. Soc.* 163 (2016) D757–D763.
- [24] M.V. Smirnov, V.Y. Kudyakov, Complexing in molten mixtures of thorium and alkali-halides, *Electrochim. Acta* 28 (1983) 1349–1359.